Research in Astron. Astrophys. **2010** Vol. **10** No. **5**, 473–483
http://www.raa-journal.org *http://www.iop.org/journals/raa*

Research in Astronomy and Astrophysics

Relationship between CME dynamics and solar flare plasma

Rajmal Jain[1], Malini Aggarwal[1] and Pradeep Kulkarni[2]

[1] Physical Research Laboratory, (Deptartment of Space, Government of India), Navrangpura, Ahmedabad – 380 009, India; *rajmal@prl.res.in, asmalini@rediffmail.com*
[2] Deptartment of Physics, Z. B. Patil College, North Maharashtra University, Jalgaon, India

Received 2009 July 17; accepted 2010 February 9

Abstract The relationship between the velocity of CMEs and the plasma temperature of the associated X-ray solar flares is investigated. The velocity of CMEs increases with plasma temperature ($R = 0.82$) and photon index below the break energy ($R = 0.60$) of X-ray flares. The heating of the coronal plasma appears to be significant with respect to the kinetics of a CME from the reconnection region where the flare also occurs. We propose that the initiation and velocity of CMEs perhaps depend upon the dominant process of conversion of the magnetic field energy of the active region to heating/accelerating the coronal plasma in the reconnected loops. Results show that a flare and the associated CME are two components of one energy release system, perhaps, magnetic field free energy.

Key words: Sun: corona — Sun: coronal mass ejections (CMEs) — Sun: flares

1 INTRODUCTION

The relationship between solar flares and Coronal Mass Ejections (CMEs) is a big issue in solar physics (e.g., Gosling 1993; Hudson et al. 1995). Both of these phenomena often occur in conjunction but the relationship is not one to one; the exact nature of the flare and CME triggers and the relationship between the cause and consequence is still open and quite puzzling. Kahler (1992) pointed out that if the CME is associated with a flare then the CME originates in the explosive phase of the flare and such flares are long-decay events (LDEs); but the relationship of CMEs with impulsive flares is still unknown. At present there are three scenarios which have been proposed. In the flare-causing-CME scenario, the increase in temperature and density observed in a flare (Parker 1961) can produce a CME. In the CME-causing-flare scenario, CMEs cause flares (Kahler 1992). In the third scenario (Harrison 1995) flares and CMEs are independent consequences of the same magnetic "disease." High quality experimental observations of the solar corona (Zhang et al. 2001; Harrison & Bewsher 2007) are found to be compatible with the third, common cause scenario, but, if from one side they seem to reject the flare-causing-CME scenario, they do not definitely exclude the CME-causing-flare scenario. In the above standard approaches, the attempt is to discriminate among the possible scenarios by means of a precise localization in time and space of a CME and of eventually 'associated' flares. This is not always possible due to the absence of observations in the solar disk and lower corona. There have also been a number of statistical investigations into the properties of soft X-ray flares in general, such as temperature, emission measure (EM) and duration (Harrison 1995 and references therein). The peak emission measure and the color temperature (T),

as determined from observations by GOES, have both been found to be correlated with the peak intensity (Feldman et al. 1995, 1996) and, in addition, peak emission measures are predicted to vary as EM$\propto T^{-7}$ (Aschwanden 1999). Veronig et al. (2002) found that duration increases with peak intensity of the flare. However they do not attempt to differentiate between flares with and without associated CMEs. Kay et al. (2003) compared the flare parameters to find the relationship between solar flares with and without associated CMEs. Systematic differences in the relationship between peak temperature and intensity for the two types of events were evident, with flares associated with CMEs tending to have lower peak temperatures than non-ejective events of the same intensity. They found a correlation between peak intensity and flare duration for the events without CMEs, while no correlation is found in the case of the flares associated with CMEs, suggesting that the occurrence of a CME intrinsically affects the timescale for energy release and cooling within the flare. On the contrary, Aggarwal et al. (2008) studied the characteristics of flares with associated CMEs and found an almost linear relationship between the peak intensity and duration of the flare in soft X-rays, i.e., in 4.1–10 keV but not in 10–20 keV. They found that the velocity of CMEs increases as a function of duration of the flares in both energy bands, indicating the possibility of associating CMEs that have higher velocity with long duration flare events.

However, it has been widely accepted that both CMEs and flares are different aspects of a unified picture (Shibata 1996) though there are many remaining problems, such as what determines the CME velocity? However, it is probably related to the accelerating effect of a flux rope and decelerating effect of the overlying field (e.g., Török & Kliem 2007). There are many other studies on the statistics of CME velocities, e.g, Zhang & Dere (2006), Chen et al. (2006), and Maričić et al. (2007). In fact, a correlation between CME velocity and photospheric magnetic field parameters has been found by Chen et al. (2006). Su et al. (2007) found that both the magnetic flux of the flaring active region and the change of shear angle of the foot points of the flare showed the most significant correlations with the velocities of CMEs. The various observations indicated that CME dynamics are closely related to the energy release in the associated flare, or vice versa, and the energy release in the flare is tightly associated with the CME kinematics. For example, statistical studies show that CME parameters, like the velocity or kinetic energy, are correlated with characteristics of the associated flare, e.g., the soft X-ray (SXR) peak flux or the integrated flux (Moon et al. 2002, 2003; Burkepile et al. 2004; Vršnak et al. 2005; Chen & Zong 2009). Very recently, Jing et al. (2005) found that there is a good correlation between magnetic reconnection rates and flux rope accelerations for 10 two-ribbon flares. The above results imply that there exist close physical connections between CME kinematics and flaring processes, at least for a certain class of CME-flare pairs.

However, no study has been made on the relationship between the dynamics of CMEs and the X-ray flare plasma characteristics to address the important question of whether solar flares and associated CMEs are two components of one energy release system. In this context, we study the X-ray emission characteristics of 26 flares observed by the Solar X-ray Spectrometer (SOXS) in the energy band 4–56 keV and compare them with dynamics of the associated CMEs.

This paper is arranged as follows: the data analysis and results are described in Section 2 and finally the discussion in Section 3.

2 DATA ANALYSIS AND RESULTS

The data of X-ray solar flares are acquired by using the "Solar X-ray Spectrometer (SOXS)" Low Energy Detector (SLD) onboard the GSLV D2 mission (Jain et al. 2005, 2006). SOXS aims to study the high energy and temporal resolution of X-ray spectra from solar flares. The SLD is comprised of two semiconductor devices, viz. a Silicon PIN detector (area 11.56 sq. mm) for 4–25 keV and a Cadmium Zinc Telluride (CZT) detector (area 25 sq. mm) for the 4–56 keV energy range. The solar flares chosen for this study were observed by both the Si and CZT detectors. However, in the current investigation, we have used data from the CZT detector only because it has a higher

energy range. The spectral data have 3 s cadence during quiet time and 100 ms in both temporal and spectral modes in the flare mode. The 8-bit ADC provides 0.218 keV channel width in the CZT X-ray spectrum, while the detector provides 1.8 keV resolution throughout its dynamic range. The daily X-ray observations and the preliminary light curves obtained using the CZT detector are taken from the SOXS website (*http://www.prl.res.in/∼ soxs-data/*). The solar flare observations are recorded from 0350 to 0650 UT. The SLD observations allow us to study soft and medium-hard X-ray emission characteristics of the flares, which we compare with dynamics of associated CMEs observed by EIT (EUV Imaging Telescope) and LASCO (Large Angle and Spectrometric Coronagraph) experiments onboard the Solar and Heliospheric Observatory (SOHO) mission.

The observations of CMEs and preliminary kinematics are taken from the LASCO/CME Catalog (available at *http://cdaw.gsfc.nasa.gov/CME_list/*). This catalog contains all CMEs manually identified since 1996 from the LASCO onboard the SOHO mission. The CMEs are detected by the LASCO coronagraphs C2 and C3, which cover a combined field of view from 2.1 to 32 Rs with a cadence of around 10–50 min. The actual increase of a CME's height (in units of Rs) with time as it expands away from the sun is available in the text file on the website. The direct and difference LASCO/C2 movies with direct and difference superposed EIT images are also linked to this site. These movies provide a complete view of the CME in question. The superposed EIT images, especially the difference images, are very useful in locating the solar sources of the CME.

Coronal dimming is widely believed to be the near-surface manifestation of CMEs (e.g., Hudson et al. 1996; Sterling & Hudson 1997; Harra & Sterling 2001), and the EIT (Delaboudiniere et al. 1995) dimming area is found to map the "foot-point" of the CME (Thompson et al. 2000; Harrison 2003). However, because the time window analysis by itself could produce false flare-CME pairs, we checked the consistency of the associations by viewing both flare and CME movies in the catalog. To get a sample of CMEs originating in the front side, the EIT running-difference movies were examined carefully. Only the CMEs that are associated with EIT dimmings appearing almost in the same angular span during their propagation in the LASCO/C2 field of view were selected in the present study.

The onset time is the most basic parameter to investigate the relation between flares and CMEs. Onset times of CMEs are difficult to identify since they originate below the LASCO C2 field of view (FOV). Exceptions are the CMEs observed by LASCO C1 (e.g. Gopalswamy & Thompson 2000; Zhang et al. 2001). These studies showed that the onsets of the flares and CMEs are tightly connected. However, this kind of data is not available for the majority of the CMEs, so the CME onset is either estimated from CME-related surface activities (e.g., filament eruptions) or is extrapolated to the solar surface from the CME trajectory in the LASCO C2 and C3 FOVs. We attempted to examine the temporal relationship using the extrapolated CME onset.

First, we selected the CMEs that are associated with flares in both timing and spatiality. For this, we scanned the LASCO images of a given CME plus the SOXS X-ray time profiles to identify unambiguously the flare-CME association. For the flare event time, we take the start time of the flare when the flux becomes 3σ above the background flux in the CZT detector, where σ is the standard deviation of the pre-flare background. It is also known that soft X-ray emission from the flare begins in an early stage at the reconnection site of the loops generally in the lower corona i.e., 10^4-10^5 km above the photosphere. Because the CME is spatially displaced from the position where the flare can be observed due to constraints on observing the CME in the lower corona, hence the timing of an observed CME is also displaced from the flare onset time. Zhang et al. (2001) investigated the initial phase of well-observed limb CMEs using the data of EIT and the LASCO C1 onboard SOHO and the GOES flare data. They demonstrated that the impulsive acceleration phase of the CMEs coincides very well with the rising phase of the associated soft X-ray flares. As the events considered in the current study do not have C1 LASCO observations, we have made observations with C2 and C3 telescopes starting at 2–4 solar radii by making at least two assumptions to obtain the extrapolated onsets. The first is the shape of a CME trajectory under the occulting disk. We assume that the

unseen trajectory is the same as observed in the LASCO FOVs. In the case of CMEs with constant speed or deceleration motion, the above assumption is apparently incorrect since all CMEs must have an acceleration phase during their initiation. Ignoring the acceleration phase, the extrapolated onsets would be later than the actual onsets. The second necessary assumption is regarding the position where the CME is initiated. We assume that the apex of the CMEs starts from 1.1 Rs. Flare position is a good proxy, but the spatial size of CMEs at the beginning would be larger than that of flares. Ignoring the spatial size of the CMEs, for the limb events, the extrapolated onsets would be earlier than the actual CME onsets. Thus, in the current investigation, an attempt to identify the association of flare and CME events from the observations on temporal and spatial scales with the best possibility has been made. The height of the CME observed by C2 and C3 coronagraphs is plotted with time for each CME and fitted by linear or second order relations, whichever is better, as shown in Figure 1 (top panel). The event onset time of a CME is defined to be the time it reaches 1.1 Rs and is determined by a backward extrapolation from the first appearance time in C2 with the use of the fitting to the height-time curve. The determination of the event time unavoidably suffers a significant error if the CME initiates away from the limb or if the CME undergoes a very different acceleration in the inner corona than in the instrumental field of view (Moon et al. 2002; Yashiro et al. 2005). At the bottom (cf. Fig. 1), the X-ray time profile of the associated flare observed by SOXS in 4.1–10 keV is plotted (cf. Fig. 1), which enabled us to correlate the onset time with that of the CME. To further confirm their association, wherever it was possible, we looked at EIT images of the CME and flare to confirm that their origin was in the same Active Region (AR). Based on this technique, a total of 26 flares (observed by SOXS) with front-side CMEs, shown in Table 1, obtained during June 2003 to December 2006, were found to be associated with CMEs and considered here.

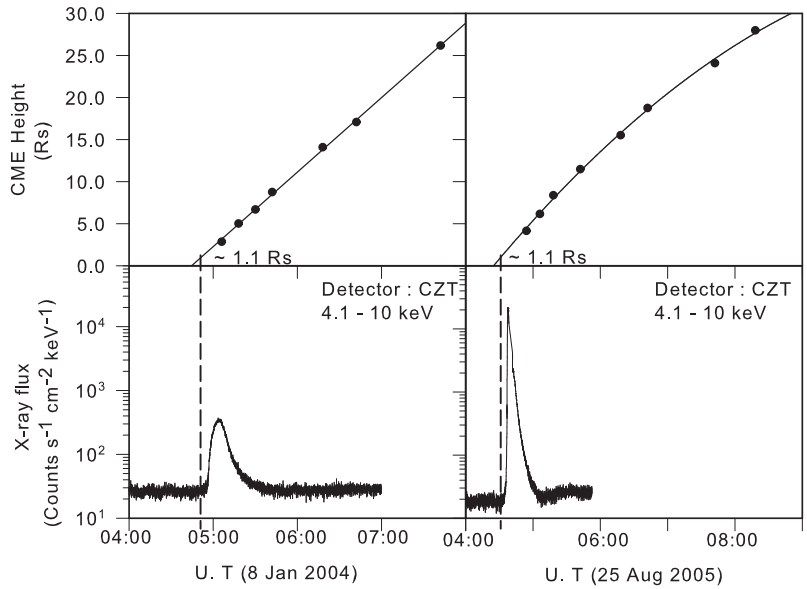

Fig. 1 Schematic representation of CME-flare association on a temporal scale for two events, 2004 Jan 8 (*left*) and 2005 Aug 25 (*right*). The height of the CME observed by LASCO instruments C2 and C3 (*top panel*) and X-ray flux of the associated flare in the 4.1–10 keV band (*bottom panel*) are plotted as a function of time. The observed CME heights are fitted with linear (*left*) or second order relations (*right*) and extrapolated to 1.1 Rs from the center of the Sun to determine the CME onset time in the corona where the soft X-ray flare also occurs.

Our technique to examine the association between the flare and CME (cf. Fig. 1) enabled us to conclude, within the temporal cadence limits of the LASCO instruments and the spatial resolution limits of the imaging instruments onboard SOHO, that the onset time of the flare and associated CME in the current investigation is very close ($\pm$ 40 min). Table 1 lists the physical parameters of X-ray flares (peak flux, start time, peak time and end time) as observed by the CZT detector in 4.1–10 keV of SOXS and associated CMEs as observed by LASCO/SOHO respectively. The peak flux in Table 1 is the maximum flux obtained by taking the average of the measured counts in 100 ms intervals in the flare mode and the corresponding time is the peak time of the flare. The end time is the time where the intensity of the flare returned to the pre-flare background or where it leveled off, whichever occurred earlier. The locations of flares can be determined from EIT images as well as from Solar Geophysics Data Reports which are based on ground-based optical Hα imaging observations. From Table 1, we found a total of 2, 13 and 11 flares of B, C and M class importance respectively associated with CMEs, which reveals that not only large but also small flares are associated with CMEs. This is in agreement with previous studies by many other investigators (e.g. McAllister et al. 1996). The onset time difference between CMEs and associated flares is of great significance in that it can provide a clue as to which is a driver of the other. In this view, we found that in 62% of the cases, the CME occurs before the flare. This is in agreement with Hundhausen (1999) who showed the close temporal relation between CMEs and flares, and suggested that flare onset lags behind the CME onset by at least a few minutes. The mean value of the onset time difference between the CMEs and the associated flares based on the linear CME speed (first order) or constant acceleration (second order) method is –5 min. This suggests that when these events are associated, there might be a common source of energy, for example magnetic field energy, which is released via reconnection (Hudson et al. 1995), however, it may be at a different altitude. However, in order to investigate this aspect, we analyzed the X-ray emission characteristics of the flare in contrast with the dynamics of the CMEs during the rise phase of the flare.

We analyzed the energy spectra observed by the CZT detector to derive plasma parameters of the flares such as temperature, emission measure, and spectral index using the OSPEX spectra fitting program. This program takes its main routine from Solarsoft where the Mewe and CHIANTI codes are included. The instrumental response function for both Si and CZT detectors are included in the SolarSoft package for SOXS to enable forward fit of the count spectra. The temperature in the flare plasma varies during its evolution in general and during the rise time in particular (Jain et al. 2006). Therefore, the flare plasma cannot be considered isothermal for the period of integration of the spectra of about one minute. Thus we consider the multi-thermal power-law for thermal plasma and the broken power-law for thermal and non-thermal continuum using the CHIANTI codes (cf. Fig. 2) for fitting to the observed spectra of the flare. For this we form the count spectrum by integrating the high cadence spectra over one minute and do a forward fit for the energy range of interest at one time by a best-fit to the curve features based on the minimum reduced χ^2 (difference counts) technique (Jain et al. 2006). We especially chose the count spectra of the flare during the rise phase considering that the two events (CME-flare) occurred simultaneously. In the multi-thermal power-law, the minimum coronal plasma temperature is considered to be constant=0.5 keV, while the maximum plasma temperature is a free parameter, determined by the best-fit. The broken power-law function with/without discontinuities in the derivatives obtain: normalization at E-pivot; break energy, negative power law index below (γ_1) and above break energy (γ_2). The break energy is kept constant at 12 keV in view of the fact that the low energy cut-off of non-thermal continuum emission is not precisely known, and varies between 10–20 keV during early evolution of the flare. Further, during the rise time, thermal continuum also contributes significantly in many flares.

The fitted count spectrum is de-convolved over the response of the instrument to obtain the photon spectrum as shown in Figure 2. As an example, the photon spectrum for the 2005 August 25 flare event during the rise time from 04:35:30 to 04:37:00 UT in 4.0–56 keV is shown. The spectral fits using the multi-thermal (green) and broken power-law (yellow) mechanisms in the energy range

Table 1 Physical Properties of Flares and Associated CMEs

	Flare Characteristics							CME Characteristics			
S. No.	Date	Start time	Peak time	End time	Peak flux	GOES	Location	Onset time at 1.1 Rs	Central PA (deg.)	Angular width (deg.)	Linear Velocity (km s^{-1})
1	13 Nov. 03	04:58:57	05:01:48	05:15:49	1157.8	M1.6	N01E90	04:39:24	103	62	598
2	07 Jan.04	03:56:41	04:01:12	04:45:00	3918.2	M4.5	N02E76	03:53:24	78	171	1581
3	08 Jan.04	04:56:53	05:03:00	05:34:42	343.2	M1.3	N03E63	04:52:48	83	144	1713
4	05Apr.04	05:31:20	05:50:57	06:35:29	1595.7	M1.7	S18E35	05:38:18	111	191	608
5	11Apr.04	04:00:31	04:08:44	04:56:25	98.970	C 9.6	S16W46	04:08:22	203	314	1645
6	31May.04	04:22:47	04:29:27	04:51:07	35.980	C2.3	S12W80	04:13:56	250	41	158
7	16Jun.04	04:25:41	4:33:03	04:58:01	41.920	C2.8	S06E81	03:56:11	72	127	603
8	21Jul.04	04:46:56	04:57:47	05:02:37	14.610	C8.9	N04E25	04:50:42	165	66	419
9	12Aug.04	04:41:26	04:58:42	05:17:33	36.970	M1.2	S15W00	04:22:12	198	115	176
10	19Aug.04	04:23:46	04:26:34	04:42:40	17.590	C4.0	N10E90	04:04:57	103	39	279
11	31Aug.04	05:28:53	05:35:31	05:51:57	352.70	M1.4	N06W82	05:05:43	272	70	311
12	09Sep.04	04:59:44	05:14:38	06:04:40	22.030	C3.2	N01E89	04:52:45	101	52	257
13	23Oct.04	03:53:10	04:00:05	04:05:25	66.080	C1.8	N16E81	04:35:20	99	61	468
14	31Oct.04	05:25:26	05:31:02	05:54:04	4200.1	M2.3	N12W36	04:44:34	251	62	265
15	29Dec.04	05:48:16	05:51:50	05:58:33	42.390	C4.9	S11W90	05:21:13	227	41	563
16	1Jul.05	04:58:32	05:01:44	05:07:51	152.53	C5.3	N14E83	04:43:16	78	42	419
17	12Jul.05	04:18:36	04:28:19	04:38:19	19.800	B6.0	N12W84	04:26:19	280	34	711
18	14Jul.05	04:23:36	04:34:05	04:45:00	28.270	C2.2	N10W90	04:42:28	252	14	560
19	27Jul.05	04:46:32	04:53:34	05:30:22	533.72	M3.7	N11E90	04:44:24	Halo	360	1787
20	03Aug.05	04:56:42	05:04:12	05:24:50	3804.4	M3.4	S13E45	04:54:03	104	65	479
21	25Aug.05	04:34:34	04:39:25	05:04:11	7331.1	M6.4	N09E80	04:31:48	115	146	1327
22	12Oct.05	05:37:07	05:40:44	05:50:24	15.950	C1.2	S10W14	05:03:54	269	69	228
23	15Jun.06	04:18:44	04:22:58	04:37:37	122.69	C2.6	S05W90	03:45:34	271	61	178
24	30Jul.03*	04:07:52	04:09:39	04:29:18	3826.5	M2.5	N14W56	04:39:36	56	9	589
25	26Jun.04*	04:18:45	04:22:48	04:30:54	26.700	C1.3	S10E86	04:37:34	250	69	775
26	03Nov.05	04:33:57	04:44:13	04:53:37	14.120	B9.1	unknown	04:51:53	156	77	304

* - Identification is not unambiguous.

4.1–2730 keV, and their total (red) fit to the observed spectrum (black) are shown. The residual after fitting is shown in the bottom panel. The thermal and non-thermal continuum spectrum can be approximated by a double power-law with spectral indices, γ_1=3.57 and $\gamma_2 = 2.91$. The thermal spectrum that dominates ≤ 9 keV and continuum (γ_1) below break energy (12 keV) corresponds to a temperature of 17 MK (1.46 keV). In this way, the maximum plasma temperature of solar flare plasma is obtained for all 26 considered flares.

Figure 3 shows a scatter plot of velocity of the CMEs as a function of plasma temperature of the solar flare obtained from the fitted spectra. Though the CZT detector restricts the temperature measurements to ± 1 channel (± 2.3 MK), the observed correlation is 0.82. This suggests that when the free magnetic field energy in the active region gets converted predominantly to heating the flare plasma near the energy release site then the associated outgoing CME initially moves faster as shown clearly from Figure 3. This also suggests that the source of energy release of both events when they are associated is the same. On the other hand, the power law index below break energy (γ_1) and the power law index above break energy (γ_2) obtained from the broken power-law fit correspond to continuum X-ray emission, which may arise from thermal and/or non-thermal bremsstrahlung processes. The velocity of the CMEs as a function of power law index below break energy (γ_1) of the associated flare is shown in Figure 4. The CME's velocity increases exponentially with γ_1 ($R = 0.60$, where R is the correlation coefficient), which mainly refers to the thermal continuum. This again suggests that the coronal flare plasma temperature may play an important role in governing the velocity of the associated CMEs. On the contrary, when we looked into γ_2, no significant relationship is found with

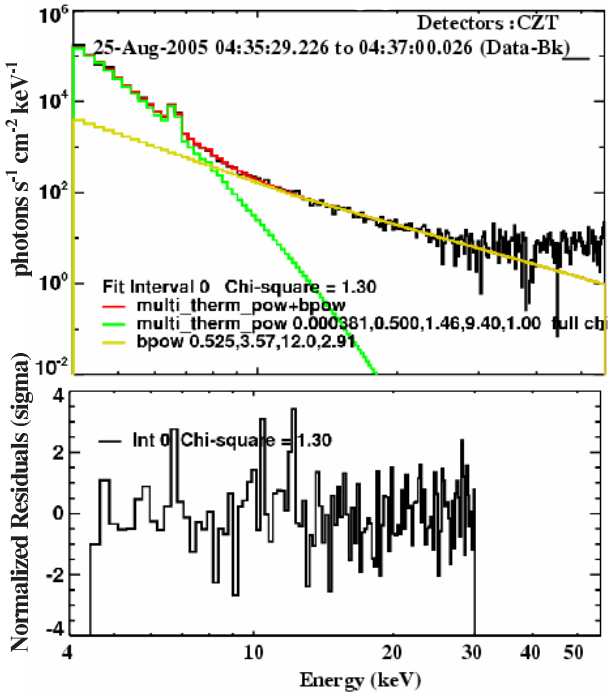

Fig. 2 Photon spectrum (*top panel*) of the 2005 August 25 flare derived from the forward fit of the count spectrum integrated over a time interval from 04:35:30–04:37:00 UT during the rise period. The observed spectrum is fitted with multi-thermal and broken power-law assumptions. The residuals to the fit are shown in the bottom panel.

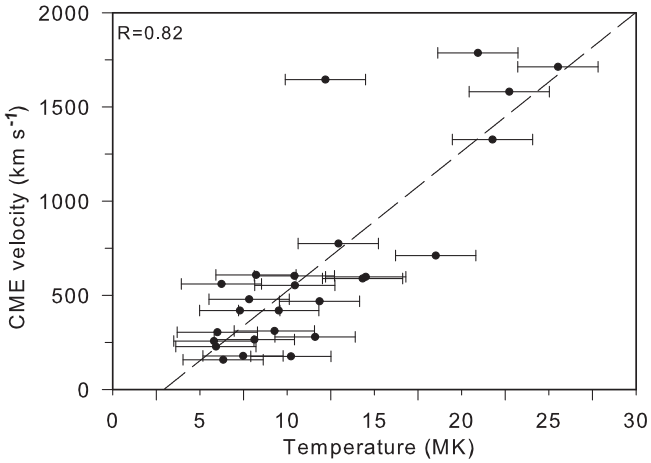

Fig. 3 Velocity of the CMEs as a function of the flare plasma temperature during the evolution. CZT detector restricts temperature measurements to an uncertainty of ± 2.3 MK.

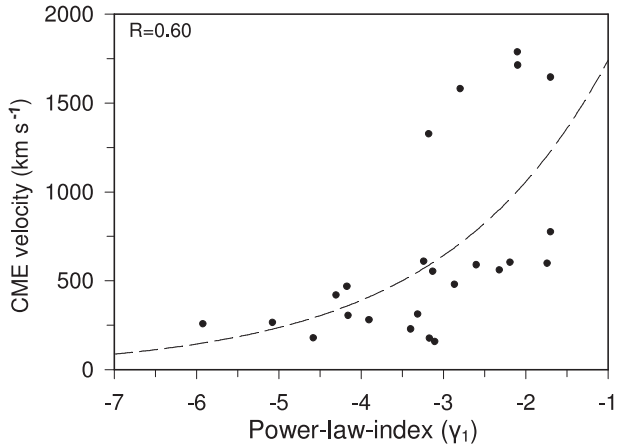

Fig. 4 Velocity of the CMEs as a function of power-law photon index below the break energy (γ_1) derived from the broken power-law fit to the X-ray spectra of the associated flares.

the initial velocity of CMEs, which refers to the contribution from non-thermal continuum, though by and large it appears that velocity of the CMEs reduces with an increase in γ_2. This conclusion needs further verification using a large sample of events.

3 DISCUSSION

It is well known that solar flare energy comes from sudden release of free magnetic energy via magnetic reconnection. In commonly adopted flare models, the ever-ascending Y-type reconnection point in the solar corona results in expanding flare loops and separation motion of flare footpoints, whereas, coronal mass ejections (CMEs) are initiated in the solar corona, which is dominated by magnetic energy, and therefore their energy source must be magnetic. However, flares could provide enough heat energy to the CME, and flares get their energy from the magnetic field anyway. Thus, the energy source for flares and CMEs is considered to be magnetic field energy except that energy release mechanisms may be different for these two events. Svestka (1986) demonstrated that in CMEs associated with flares and those without flares, the cause of the CME is the same: an opening of magnetic field lines, which were previously closed in the form of arcades or helmet streamers along the polarity inversion line of the longitudinal magnetic field; the only difference between flare-associated and non-flare-associated CMEs is the strength of the magnetic field in the region where the opening takes place.

From Table 1, we found that the onset time of CMEs is earlier (in 62% of cases) than the onset time of the flares by tens of minutes. The mean value of the onset time difference between the CMEs and the associated flares based on the linear CME speed (first order) or constant acceleration (second order) method is –5 min; that is, the CME preceded the flares by about 5 min which is consistent with Andrews (2002). From his investigation, he argued that the CME launch and the flare start are simultaneous with an uncertainty of several minutes. Our results based on the constant speed method lead to a similar conclusion. According to Yashiro & Gopalswamy (2008), the difference between flare and CME onsets shows a Gaussian distribution with standard deviation σ= 17 min (σ= 15 min) for the first (second) order extrapolated CME onset. Therefore, it is reasonable to consider that the difference between the flare and extrapolated CME onsets results not from the nature of the flare-

CME relation but from the error of the extrapolated CME onset. According to Zhang et al. (2001), using LASCO C1 observations showed that the onset of the accompanying flare largely marks the end of the initiation phase but marks the onset of the impulsive acceleration phase. Our results using LASCO C2 and C3 support an idea that the initiation of most CMEs precedes the onset of the associated flares seen in soft X-rays. In a statistical sense, this result seems to be consistent with Harrison and his colleagues (Harrison et al. 1990) who found that the CME initiation is timed 10 to 20 min before the start of hard X-ray flaring and is nearly coincident with the preflare phase. Moon et al. (2005) studied the CME-flare events from the LASCO C1 coronagraph or loop displacements seen in SOHO/EIT and TRACE images without any extrapolation and found that the onset time difference for these events in most cases (about 80%) is such that the CME initiation precedes the onset of the associated flare. These facts simply reject the view that the flare is the cause of the CME. On the other hand, however, we cannot simply conclude that the CME is the cause of the flare. This led us to conclude in the first instance that both flare and CME are perhaps triggered by one mechanism. This is in agreement with Hundhausen (1999) who showed the close temporal relation between CMEs and flares, and suggested that flare onset lags behind the CME onset by at least a few minutes.

It has been widely accepted that a flare is caused by the magnetic reconnection process, which rapidly dissipates the magnetic energy prestored in the corona. Nonthermal energetic particles are accelerated inside or in the vicinity of the reconnection region through various possible mechanisms (review by Priest & Forbes 2002). Our study unambiguously revealed evidence of a relationship between the velocity of CMEs and the peak plasma temperature during the rise time of the solar flare. Though the strong correlation between the two is not suggestive of a causal relationship but rather both might be a bi-product of a common trigger such as the magnetic field energy stored in the solar atmosphere. The initiation phase of CMEs may be caused by the destabilization and quasi-static evolution, and violent magnetic activity may be triggered that induces the magnetic force to drive CMEs, while simultaneously accelerating particles or heating the plasma to cause flares. In this scenario, CMEs and flares are two different manifestations of the same magnetic process in the corona; they have a strongly coupled relationship but not a cause-effect one. It appears to us that the same single energy release system is responsible in the coronal plasma at the point of reconnection of the loops which, when heated during the early rise phase of the flare, which is determined by the balance between reconnection heating and conduction cooling (Yokoyama & Shibata 2001), also determines the velocity of the outgoing CME.

In contrast, instead of heating the coronal plasma, if excess particle acceleration takes place during reconnection producing hard X-ray emission in the solar flares then the velocity of the associated CME may be smaller. Our results also propose the possibility of a significant role of heating of the coronal plasma in governing the CME velocity. However, Török & Kleim (2007) concluded that increased magnetic complexity is reflected in steep magnetic gradients in the source AR's corona, producing faster CMEs. Also Venkatakrishnan & Ravindra (2003) concluded that it is the magnetic energy of the AR that drives the CME. The restructuring of the AR field lines in the corona, which can push material with Alfven speed and thus inject energy into the plasma on a time scale shorter than the dynamical time of the corona, is considered to be the likely process that can drive the CME. Chen et al. (2006) found that for filament-associated CMEs, the velocity of CME V_{CME} is also roughly linearly correlated with the total magnetic flux in the filament channel. However, they found that the correlation between V_{CME} and the average magnetic field in the filament channel is better. The magnetic field energy is converted in the corona during reconnection into heating the plasma and accelerating the particles. Our measurements showed a strong relationship between the flare plasma temperature and the velocity of CME, and thereby appear to show evidence in view of the magnetic field strength of the AR. Therefore, we propose that the speed of CMEs perhaps depends upon the dominant process of conversion of the magnetic field energy to heating or accelerating the coronal plasma in the reconnected loops, which is in close agreement with Zhang & Dere (2006).

Acknowledgements Authors thank Prof. B. R. Dennis, Dr. R. Schwartz and Ms. Kim Tolbert, GSFC for their valuable advices and developing the software for SOXS analysis. We also acknowledge Prof. N Gopalswamy for the fruitful suggestions. The CME website is highly acknowledged. We thank the anonymous referee for helpful suggestions and constructive comments that improved the manuscript.

References

Aggarwal, M., Jain, R., Mishra, A. P., Kulkarni, P. G., Vyas, C., Sharma, R., & Gupta, M. 2008, Journal of Astrophysics and Astronomy, 29, 195

Andrews, M. D. 2002, Characteristics of CMEs associated with big flares, in Solar Variability: From Core to Outer Frontiers, The 10th European Solar Physics Meeting, 9-14 September 2002, Prague, Czech Republic, ed. A. Wilson (ESA Spec. Publ. SP-506), 2, 531

Aschwanden, M. J. 1999, Sol. Phys., 190, 233

Burkepile, J. T., Hundhausen, A. J., Stanger, A. L., St. Cyr, O. C., & Seiden, J. A. 2004, J. Geophy. Res. (Space Physics), 109, 3103

Chen, A. Q., Chen, P. F., & Fang, C. 2006, A&A, 456, 1153

Chen, A.-Q., & Zong, W.-G. 2009, RAA (Research Astron. Astrophys.), 9, 470

Delaboudinière, J.-P., et al. 1995, Sol. Phys., 162, 291

Feldman, U., Doschek, G. A., Mariska, J. T., & Brown, C. M. 1995, ApJ, 450, 441

Feldman, U., Doschek, G. A., Behring, W. E., & Phillips, K. J. H. 1996, ApJ, 460, 1034

Gopalswamy, N., & Thompson, B. J. 2000, Journal of Atmospheric and Solar-Terrestrial Physics, 62, 1457

Gosling, J. T. 1993, J. Geophys. Res., 98, 18937

Harra, L. K., & Sterling, A. C. 2001, ApJ, 561, L215

Harrison, R. A., Hildner, E., Hundhausen, A. J., Sime, D. G., & Simnett, G. M. 1990, J. Geophys. Res., 95, 917

Harrison, R. A. 1991, Royal Society of London Philosophical Transactions Series A, 336, 401

Harrison, R. A. 1995, A&A, 304, 585

Harrison, R. A. 2003, Advances in Space Research, 32, 2425

Harrison, R. A., & Bewsher, D. 2007, A&A, 461, 1155

Hudson, H., Haisch, B., & Strong, K. T. 1995, J. Geophys. Res., 100, 3473

Hudson, H. S., Acton, L. W., & Freeland, S. L. 1996, ApJ, 470, 629

Hundhausen, A. 1999, Coronal Mass Ejections, The many faces of the sun: a summary of the results from NASA's Solar Maximumn Mission. eds. K. T. Strong, J. L. R. Saba, B. M. Haisch, & J. T. Schmelz (New York: Springer), 143

Jain, R., et al. 2005, Sol. Phys., 227, 89

Jain, R., Pradhan, A. K., Joshi, V., Shah, K. J., Trivedi, J. J., Kayasth, S. L., Shah, V. M., & Deshpande, M. R. 2006, Sol. Phys., 239, 217

Jing, J., Yurchyshyn, V., Qiu, J., Xu, Y., & Wang, H. 2005, AGU Spring Meeting Abstracts, A3

Kahler, S. W. 1992, ARA&A, 30, 113

Kay, H. R. M., Harra, L. K., Matthews, S. A., Culhane, J. L., & Green, L. M. 2003, A&A, 400, 779

Maričić, D., Vršnak, B., Stanger, A. L., Veronig, A. M., Temmer, M., & Roša, D. 2007, Sol. Phys., 241, 99

McAllister, A. H., Dryer, M., McIntosh, P., Singer, H., & Weiss, L. 1996, J. Geophys. Res., 101, 13497

Moon, Y.-J., Choe, G. S., Wang, H., Park, Y. D., Gopalswamy, N., Yang, G., & Yashiro, S. 2002, ApJ, 581, 694

Moon, Y.-J., Choe, G. S., Wang, H., Park, Y. D., & Cheng, C. Z. 2003, Journal of Korean Astronomical Society, 36, 61

Moon, Y.-J., Cho, K.-S., Chae, J., Choe, G. S., Kim, Y.-H., Bong, S.-C., & Park, Y.-D. 2005, J. Geophys. Res. (Space Physics), 110, 7103

Parker, E. N. 1961, ApJ, 133, 1014

Priest, E. R., & Forbes, T. G. 2002, A&A Rev., 10, 313
Shibata, K. 1996, Advances in Space Research, 17, 9
Sterling, A. C., & Hudson, H. S. 1997, ApJ, 491, L55
Su, Y., Van Ballegooijen, A., McCaughey, J., Deluca, E., Reeves, K. K., & Golub, L. 2007, ApJ, 665, 1448
Svestka, Z. 1986, in The Lower Atmosphere of Solar Flares, ed. D. F. Neidig (Tucson: Univ. Arizona Press), 332
Thompson, B. J., Cliver, E. W., Nitta, N., Delannée, C., & Delaboudinière, J.-P. 2000, Geophys. Res. Lett., 27, 1431
Török, T., & Kliem, B. 2007, Astronomische Nachrichten, 328, 743
Venkatakrishnan, P., & Ravindra, B. 2003, Geophys. Res. Lett., 30, 230000
Veronig, A., Temmer, M., Hanslmeier, A., Otruba, W., & Messerotti, M. 2002, A&A, 382, 1070
Vršnak, B., Sudar, D., & Ruždjak, D. 2005, A&A, 435, 1149
Yashiro, S., Gopalswamy, N., Akiyama, S., Michalek, G., & Howard, R. A. 2005, J. Geophys. Res. (Space Physics), 110, 12
Yashiro, S., & Gopalswamy, N. 2008, Statistical Relationship between Solar Flares and Coronal Mass Ejections, Universal Heliophysical Processes, Proceedings IAU Symposium No. 257, eds. N. Gopalswamy, & D. Webb
Yokoyama, T., & Shibata, K. 2001, ApJ, 549, 1160
Zhang, J., Dere, K. P., Howard, R. A., Kundu, M. R., & White, S. M. 2001, ApJ, 559, 452
Zhang, J., & Dere, K. P. 2006, ApJ, 649, 1100